Supplementary materials

Multi-level chiral edge states in Janus $M_2XS_2Se_2$ (M = V, Ti; X = W, Mo) monolayers with high Curie temperature and sizable nontrivial topological gaps

Li Deng[a], Xiang Yin[a], Yanzhao Wu[a], Junwei Tong[b], Gaowu Qin[a] and Xianmin Zhang[a]*
[a]Key Laboratory for Anisotropy and Texture of Materials (Ministry of Education), School of Material Science and Engineering, Northeastern University, Shenyang, 110819, China
[b]Department of Physics, Freie Universität Berlin, Berlin, 14195, Germany

Using $Ti_2WS_2Se_2$ monolayer as an example, the convergence tests of k-points and cutoff energy are conducted, as shown in Figure S1. It can be found that as the k-points and cutoff energy reaching 15×15×1 and 500 eV, the energy of $Ti_2WS_2Se_2$ monolayer become the lowest and stable. Therefore, the k-points and cutoff energy are set as 15×15×1 and 500 eV, respectively.

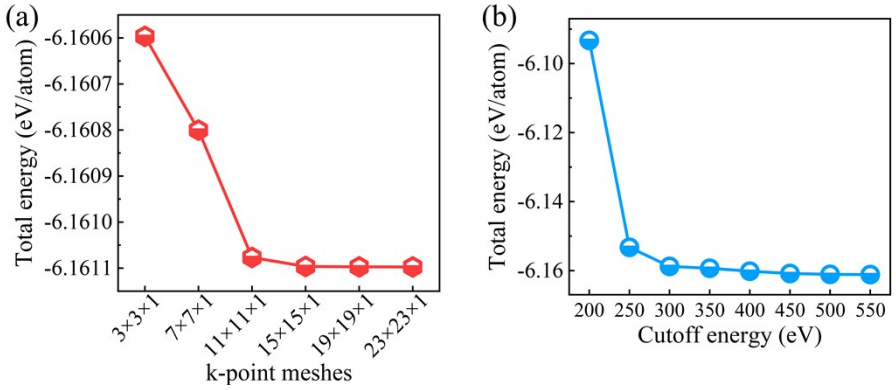

Figure S1. Convergence tests of (a) k-points and (b) cutoff energy for the $Ti_2WS_2Se_2$ monolayer.

Table S1. Lattice constant *a*, bond length *d*, monolayer thickness *h*, cohesive energy E_{coh}, and formation energy E_{form} of the $M_2XS_2Se_2$ (M = V, Ti; X = W, Mo) monolayers.

System	*a* (Å)	$d_{M\text{-}S}$ (Å)	$d_{M\text{-}Se}$ (Å)	$d_{X\text{-}S}$ (Å)	$d_{X\text{-}Se}$ (Å)	*h* (Å)	E_{coh} (eV/atom)	E_{form} (eV/atom)
$V_2WS_2Se_2$	5.83	2.42	2.55	2.30	2.45	2.74	4.93	-0.65
$V_2MoS_2Se_2$	5.82	2.40	2.53	2.32	2.46	2.71	3.56	-0.71
$Ti_2WS_2Se_2$	5.79	2.44	2.57	2.33	2.48	2.88	4.98	-0.67
$Ti_2MoS_2Se_2$	5.80	2.42	2.55	2.37	2.50	2.80	4.63	—

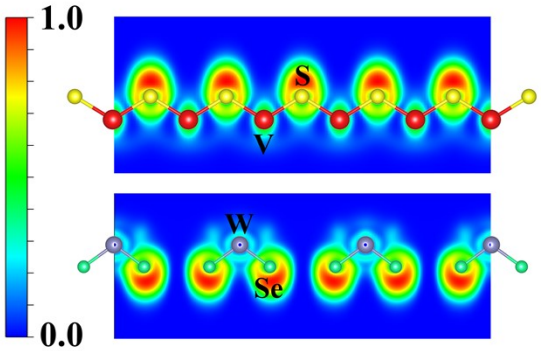

Figure S2. Electron localization function of $V_2WS_2Se_2$ monolayer in the $(1\bar{1}0)$ plane along V-S (upper)

and W-Se (lower) bonds.

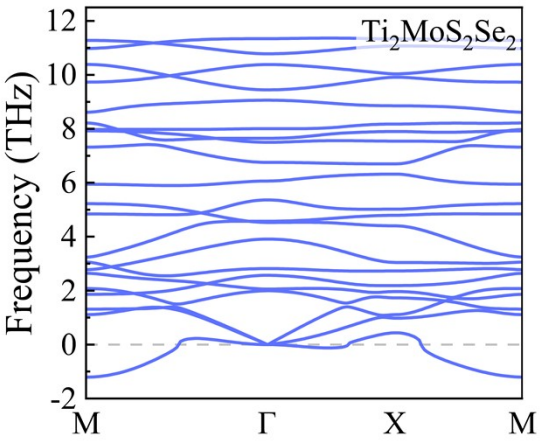

Figure S3. Phonon spectrum of the $Ti_2MoS_2Se_2$ monolayer.

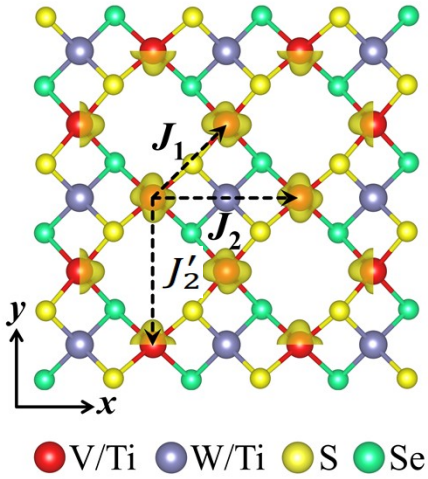

Figure S4. Spin density distribution of FM configuration and schematic of exchange parameters $(J_1, J_2 \text{ and } J_2^{'})$ for the $M_2XS_2Se_2$ (M = V, Ti; X = W, Mo) monolayers. Yellow iso-surfaces (0.03 e/bohr^3) represent the spin-up densities.

Table S2. Exchange energy ($\Delta E_{ex} = E_{AFM1/AFM2/AFM3} - E_{FM}$) of the $V_2WS_2Se_2$, $V_2MoS_2Se_2$, and $Ti_2WS_2Se_2$ monolayers.

System	E_{AMF1} - E_{FM} (meV/2 × 2 supercell)	E_{AMF2} - E_{FM} (meV/2 × 2 supercell)	E_{AMF3} - E_{FM} (meV/2 × 2 supercell)
$V_2WS_2Se_2$	1889.58	1853.46	1746.06
$V_2MoS_2Se_2$	2657.58	2087.37	2167.10
$Ti_2WS_2Se_2$	653.68	752.97	830.93

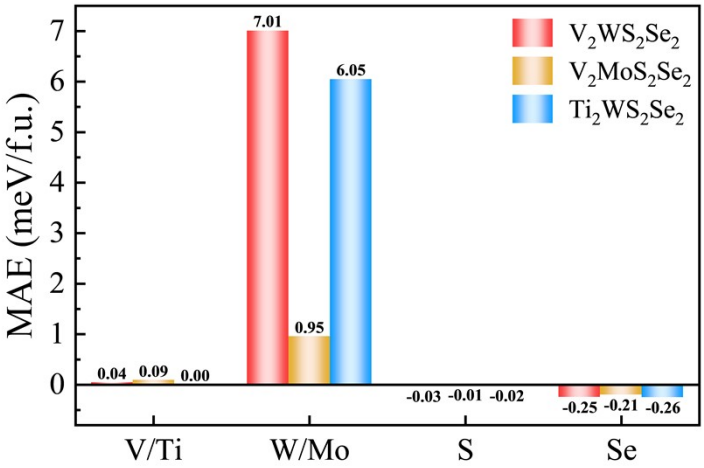

Figure S5. Atom-resolved MAE of the $V_2WS_2Se_2$, $V_2MoS_2Se_2$, and $Ti_2WS_2Se_2$ monolayers.

Table S3. Exchange parameters of the $V_2WS_2Se_2$, $V_2MoS_2Se_2$, and $Ti_2WS_2Se_2$ monolayers.

System	J_1 (meV)	J_2 (meV)	J_3 (meV)
$V_2WS_2Se_2$	26.20	22.30	2.98
$V_2MoS_2Se_2$	36.91	23.29	-2.21
$Ti_2WS_2Se_2$	20.43	26.63	4.87

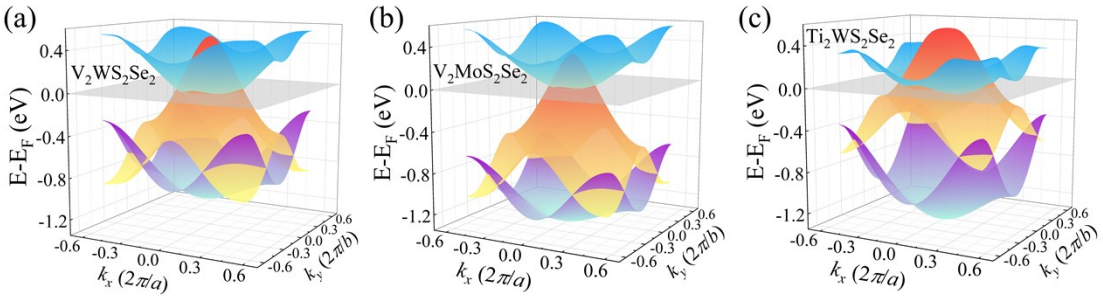

Figure S6. Three-dimensional band structures of the (a) $V_2WS_2Se_2$, (b) $V_2MoS_2Se_2$, and (c) $Ti_2WS_2Se_2$ monolayers without considering the SOC effect (only the bands related to band inversion are shown here). Red, blue, and purple bands represent the V/Ti-d_{xz},d_{yz} spin-up band, W/Mo-d_{z^2} spin-down band, and W/Mo-$d_{x^2-y^2}$ spin-down band, respectively.

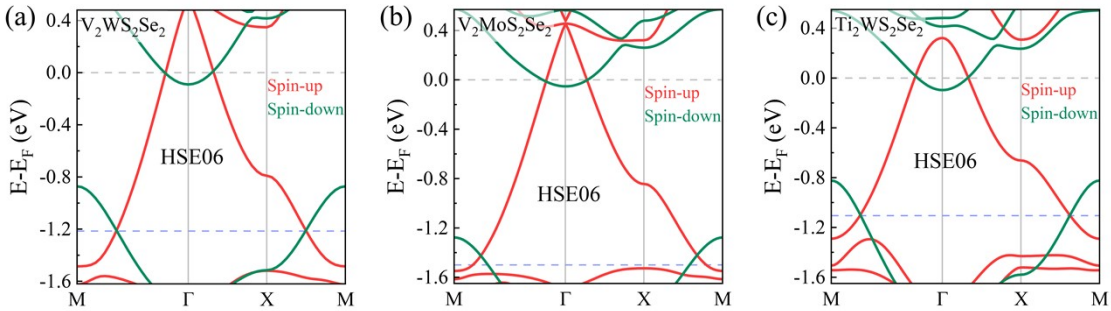

Figure S7. Spin-resolved band structures of (a) $V_2WS_2Se_2$, (b) $V_2MoS_2Se_2$, and (c) $Ti_2WS_2Se_2$

monolayers without considering the SOC effect from HSE06 method.

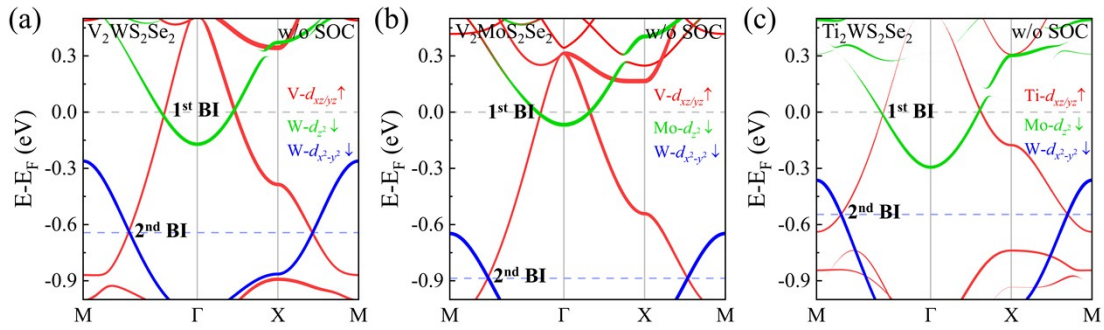

Figure S8. Orbital-resolved energy bands of the (a) $V_2WS_2Se_2$, (b) $V_2MoS_2Se_2$, and (c) $Ti_2WS_2Se_2$ monolayers with considering the SOC effect (only the bands related to band inversion are shown here).

(a) V2W1S2Se2

```
   1.00000000000000
     5.8328520454112338    0.0000000000000000    0.0000000000000000
     0.0000000000000000    5.8328520454112338    0.0000000000000000
     0.0000000000000000    0.0000000000000000   22.7435172951562379
  V    W    S    Se
     2    1    2    2
Direct
  0.0000000000000000  0.5000000000554152  0.5052295399110873
  0.5000000000554152 -0.0000000000000000  0.5052295399110873
  0.0000000000000000 -0.0000000000000000  0.5029590849258385
  0.2299054517316166  0.7700945631556890  0.5603262536924473
  0.7700945631556890  0.2299054517316166  0.5603262536924473
  0.7602784148964239  0.7602784148964239  0.4396986381781852
  0.2397215999908816  0.2397215999908816  0.4396986381781852
```

(b) V2Mo1S2Se2

```
   1.00000000000000
     5.8200015183163414    0.0000000000000000    0.0000000000000000
     0.0000000000000000    5.8200015183163414    0.0000000000000000
     0.0000000000000000    0.0000000000000000   22.7117276183695260
  V   Mo    S    Se
     2    1    2    2
Direct
  0.0000000000000000  0.5000000000554152  0.5052504299380516
  0.5000000000554152  0.0000000000000000  0.5052504299380516
  0.0000000000000000  0.0000000000000000  0.5033008025619665
  0.2345206149556347  0.7654793999316709  0.5596988407032555
  0.7654793999316709  0.2345206149556347  0.5596988407032555
  0.7570774989561642  0.7570774989561642  0.4403011592967445
  0.2429225159311414  0.2429225159311414  0.4403011592967445
```

(c) Ti2W1S2Se2

```
   1.00000000000000
     5.7896777062362244    0.0000000000000000    0.0000000000000000
     0.0000000000000000    5.7896777062362244    0.0000000000000000
     0.0000000000000000    0.0000000000000000   22.8776614447735049
  Ti   W    S    Se
     2    1    2    2
Direct
  0.0000000000000000  0.5000000000554152  0.5049520618571475
  0.5000000000554152  0.0000000000000000  0.5049520618571475
  0.0000000000000000  0.0000000000000000  0.5029973098444525
  0.2308900277787500  0.7691099871085558  0.5628779279693135
  0.7691099871085558  0.2308900277787500  0.5628779279693135
  0.7596729125889323  0.7596729125889323  0.4370703885543428
  0.2403271022983732  0.2403271022983732  0.4370703885543428
```

(d) Ti2Mo1S2Se2

```
   1.00000000000000
     5.7968949831332974    0.0000000000000000    0.0000000000000000
     0.0000000000000000    5.7968949831332974    0.0000000000000000
     0.0000000000000000    0.0000000000000000   17.7117276183695402
  Ti   Mo    S    Se
     2    1    2    2
Direct
  0.0000000000000000  0.5000000000554152  0.5070682652818640
  0.5000000000554152 -0.0000000000000000  0.5070682652818640
  0.0000000000000000 -0.0000000000000000  0.5030021382261209
  0.2382580206908854  0.7617419941964202  0.5791030809674473
  0.7617419941964202  0.2382580206908854  0.5791030809674473
  0.7509354302865990  0.7509354302865990  0.4211765124420752
  0.2490645846007066  0.2490645846007066  0.4211765124420752
```

Figure S9. The geometry of optimized structures for the (a) $V_2WS_2Se_2$, (b) $V_2MoS_2Se_2$, (c) $Ti_2WS_2Se_2$, and (d) $Ti_2MoS_2Se_2$ monolayers.